Available online at www.sciencedirect.com
ScienceDirect
Journal of Organometallic Chemistry 692 (2007) 3640–3648
Journal of Organometallic Chemistry
www.elsevier.com/locate/jorganchem

Reactions of $R_2P–P(SiMe_3)_2$ with $[(R'_3P)_2PtCl_2]$. Syntheses and structures of $[\mu_2\text{-}(1,2{:}2\text{-}\eta\text{-}P_2)\{Pt(PEt_3)_2\}_2\{Pt(PEt_3)_2Cl\}]^+Cl^-$, $[\{(Et_2PhP)_2Pt\}_2P_2]$, $[\{(p\text{-}Tol_3P)_2Pt\}_2P_2]$ and $[(p\text{-}Tol_3P)ClPt(\mu\text{-}PPh_2)_2Pt(p\text{-}Tol_3P)Cl]$

Wioleta Domańska-Babul [a], Jaroslaw Chojnacki [a], Eberhard Matern [b], Jerzy Pikies [a,*]

[a] Faculty of Chemistry, Department of Inorganic Chemistry, Gdańsk University of Technology, G. Narutowicza St. 11/12, PL-80-952 Gdańsk, Poland
[b] Institut für Anorganische Chemie, Universität Karlsruhe (TH), D-76128 Karlsruhe, Germany

Received 21 December 2006; received in revised form 8 March 2007; accepted 30 April 2007
Available online 8 May 2007

Abstract

The reactions of diphosphanes $R_2P–P(SiMe_3)_2$ (R = Ph, ^{t}Bu, Et_2N and $^i Pr_2N$) with $[(R'_3P)_2PtCl_2]$ (R'_3P=Me_3P, Et_3P, Et_2PhP, $EtPh_2P$ and p-Tol_3P) are very complex. The main reaction pathway is splitting of the P–P bond of the parent $R_2P–P(SiMe_3)_2$ followed by formation of $[\{(R'_3P)_2Pt\}_2P_2]$, $R_2P–PR_2$ and other products which have been characterized by ^{31}P NMR spectroscopy. The molecular structures of $[\{(Et_2PhP)_2Pt\}_2P_2]$, $[\{(p\text{-}Tol_3P)_2Pt\}_2P_2]\cdot 2Et_2O$, $[\mu_2\text{-}(1,2{:}2\text{-}\eta\text{-}P_2)\{Pt(PEt_3)_2\}_2\{Pt(PEt_3)_2Cl\}]^+Cl^-$ and $[(p\text{-}Tol_3P)ClPt(\mu\text{-}PPh_2)_2Pt(p\text{-}Tol_3P)Cl]$ have been determined by single-crystal X-ray structural analysis.

Keywords: P ligands; Diphosphorus complexes; Diphosphanes; Platinum; ^{31}P NMR spectroscopy; X-ray structure

1. Introduction

The reactivity of lithium derivatives of silylphosphanes and 1,2-silyl derivatives of diphosphanes towards $[(Et_3P)_2PtCl_2]$ has been a subject of thorough studies. It was established that $[(Et_3P)_2PtCl_2]$ reacts with $LiP(SiMe_3)_2$ yielding $[(Et_3P)Pt\{\mu\text{-}P(SiMe_3)_2\}_2Pt(PEt_3)]$(*Pt–Pt*), $[(Et_3P)_2Pt\{\eta^2\text{-}(PSiMe_3)_2\}]$ and $[\{(Et_3P)_2Pt\}_2P_2]$ [1]. The reaction of $^t Bu(SiMe_3)P–P(SiMe_3)_2$ with $[(Et_3P)_2PtCl_2]$ yields $[(Et_3P)_2Pt(\eta^2\text{-}^t BuP{=}PSiMe_3)]$ and the reaction of $[(Et_3P)_2PtCl_2]$ with $(SiMe_3)_2P–P(SiMe_3)_2$ yields $[(Et_3P)_2Pt(\eta^2\text{-}Me_3SiP{=}P\text{-}SiMe_3)]$ together with $[\{(Et_3P)_2Pt\}_2P_2]$. The related Ni(II) complexes with chelating tertiary phosphanes react with $R'P(SiMe_3)_2$ under formation of side-on bonded diphosphene complexes $[(dRpe)Ni\{\eta^2\text{-}(R'P{=}PR')\}]$ (dRpe = $R_2P–CH_2–CH_2–PR_2$, R = Et, ^{c}Hex and Ph) [2]. The same compounds were formed in the reactions of $[(dRpe)NiCl_2]$ with 1,2-silylated diphosphanes $(SiMe_3)R'P–P(SiMe_3)R'$ [3]. Reactions involving $P(SiMe_3)_3$ or $(SiMe_3)_2P–P(SiMe_3)_2$ yield $[\{(dRpe)Ni\}_2P_2]$ [2].

We have a long standing interest upon the chemistry of phosphinophosphinidenes $R_2P–P$ as ligands in transition metal complexes [4,5] and we successfully exploited lithiated diphosphanes $R_2P–P(SiMe_3)Li$ as precursors of $R_2P–P$ ligands. We obtained $[\mu\text{-}(1,2{:}2\text{-}\eta\text{-}^t Bu_2P{=}P)\{Zr(Cl)Cp_2\}_2]$, a complex containing both a side-on and a terminally bonded $^t Bu_2P–P$ ligand and $[(\eta^1\text{-}^t Bu_2P–P)\{Zr(PPhMe_2)Cp_2\}]$ – the first complex with this ligand terminally bonded [6]. We have extended our investigations to $^t Bu_2P–PLi–P^t Bu_2$ and established the formation of $[(1,2\text{-}\eta\text{-}^t Bu_2P{=}P–P^t Bu_2)M(PEt_3)Cl]$ (M = Ni, Pd) in the reactions with $[(Et_3P)_2MCl_2]$ (M = Ni, Pd) [7] where the triphosphorus ligand displays properties of a side-on bonded diphosphenium cation with geometry and ^{31}P NMR properties similar to the side-on bonded $^t Bu_2P–P$

* Corresponding author. Tel.: +48 58 3472622; fax: +48 58 3472694.
E-mail address: pikies@altis.chem.pg.gda.pl (J. Pikies).

0022-328X/$ - see front matter © 2007 Elsevier B.V. All rights reserved.
doi:10.1016/j.jorganchem.2007.04.045

ligand. Now we report our results upon the reactions of diphosphanes $R_2P–P(SiMe_3)_2$ with $[(R'_3P)_2PtCl_2]$ in order to study whether these compounds are able to introduce the $R_2P–P$ moiety into the Pt centre and to define the influence of the R group on the reactivity of $R_2P–P(SiMe_3)_2$.

2. Results and discussion

2.1. Reactivity

The outcomes of complicated reactions of $R_2P–P(SiMe_3)_2$ with $[(R'_3P)_2PtCl_2]$ depend very strongly upon the type of the R and R′ groups. There are many products in the reaction mixtures and in many cases we were not able to assign all the signals in the ^{31}P NMR spectra. Scheme 1 shows the main pathways of these reactions.

In the pathway **I** the P–P bond of the parent $R_2P–P(SiMe_3)_2$ is cleaved. There are significant differences in the product distributions between our reactions and the reactions of $[(Et_3P)_2PtCl_2]$ with $LiP(SiMe_3)_2$ [1]. We have not found $P(SiMe_3)_3$, $[(R'_3P)Pt\{\mu\text{-}P(SiMe_3)_2\}_2Pt(PR'_3)]$ (*Pt–Pt*), $[(Et_3P)_2Pt\{\eta^2\text{-}(PSiMe_3)_2\}]$ and $(Me_3Si)_2P–P(SiMe_3)_2$. Thus, the formation of $[(R'_3P)_2Pt\{P(SiMe_3)_2\}_2]$ in the reaction sequences seems to be very unlikely. It seems very probable, that the R_2P radical but not the $P(SiMe_3)_2$ radical was released in the reaction sequences of path **I**. It leads to phosphorus compounds (not complexes) found in the reaction mixtures. This assumption is additionally supported, because in the case of $(^iPr_2N)_2P–P(SiMe_3)_2$ the formation of $(^iPr_2N)_2PCl$ and $(^iPr_2N)_2P–P(N^iPr_2)_2$ is significantly favoured, probably due to the relative high stability of the $(^iPr_2N)_2P$ radical. The similar radical $(^iPr_2N)\{(Me_3Si)_2N\}P$ proved to be quite stable [8].

2.1.1. The ^{31}P NMR studies of the mixture obtained from the reaction of $Ph_2P–P(SiMe_3)_2$ with $[(R'_3P)_2PtCl_2]$

$Ph_2P–P(SiMe_3)_2$ reacts immediately at −40 °C after the addition of $[(R'_3P)_2PtCl_2]$ (observable by the red color of the reaction mixture). The ^{31}P NMR monitoring of the reaction mixtures is presented in Section 2.1.1. The main reaction path is **IV**. In the reaction involving $[(p\text{-}Tol_3P)_2PtCl_2]$ we isolated the phosphido-bridged complex $[(p\text{-}Tol_3P)ClPt(\mu\text{-}PPh_2)_2Pt(p\text{-}Tol_3P)Cl]$ (**4**). In the parent liquor we have not observed any ^{31}P NMR signals of **4**, probably because it is not formed in the early stages of the reactions or because of its low solubility. The parent liquor contains Ph_2PSiMe_3 resulting from splitting of the P–P bond in the $Ph_2P–P(SiMe_3)$ moiety. Thus, **4** can be the product of a reaction of Ph_2PSiMe_3 with $[(p\text{-}Tol_3P)_2PtCl_2]$ [9].

Abbreviations: (s) – strong; (m) – medium; (w) – weak; (v) – very, (b) – broad.

$Ph_2P–P(SiMe_3)_2$ (0.48 mmol), $[(Me_3P)_2PtCl_2]$ (0.24 mmol): Ph_2PH (w), $Ph_2P–P(SiMe_3)_2$ (m), $Ph_2P–PPh_2$ (m), Me_3P(s), polymer at −25 ppm (b).

$Ph_2P–P(SiMe_3)_2$ (0.30 mmol), $[(Et_3P)_2PtCl_2]$ (0.34 mmol): $Ph_2P–PPh_2$ (m), $[(Et_3P)_3PtCl]Cl$ (m), [*trans*-$(Et_3P)_2PtCl_2$] (s), Et_3P(s), **A**(m).

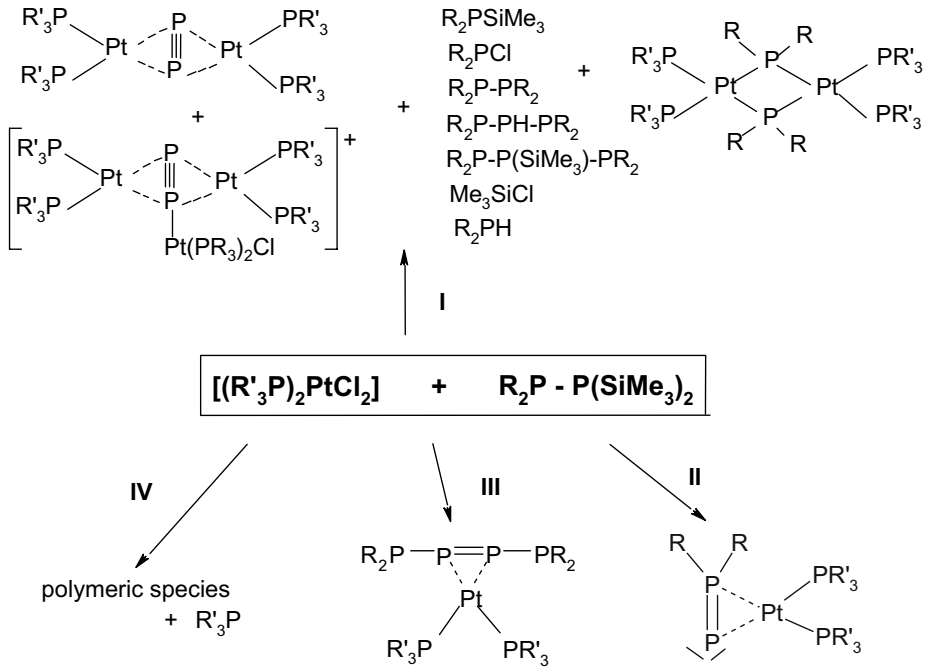

Scheme 1. The main pathways of the reactions $R_2P–P(SiMe_3)_2$ with $[(R'_3P)_2PtCl_2]$: **I** – splitting of the P–P bond of $R_2P–P(SiMe_3)_2$ and formation of diphosphorus complexes; **II** – formation of complexes with a side-on bonded phosphinophosphinidene ligand $R_2P–P$; **III** – dimerization of the $R_2P–P$ groups and formation of tetraphosphene complexes; **IV** – formation of polymeric species and release of tertiary phosphanes.

Ph_2P–$P(SiMe_3)_2$ (0.91 mmol), $[(Et_3P)_2PtCl_2]$ (0.45 mmol): Ph_2P–PPh_2 (s), Ph_2P–$P(SiMe_3)_2$ (m), $Ph_2P(SiMe_3)$ (m), $P(SiMe_3)_3$ (w), Et_3P (s), [{2,3-η-(Ph_2PP=$PPPh_2$)}$Pt(PEt_3)_2$] (m), [{$(Et_3P)_2Pt$}$_2P_2$] (s).

Ph_2P–$P(SiMe_3)_2$ (0.26 mmol), $[(Et_2PhP)_2PtCl_2]$ (0.26 mmol): Et_2PhP (vs), Ph_2P–PPh_2 (w), **B** (w), [{$(Et_2PhP)_2Pt$}$_2P_2$] (w), polymer at +10 ppm (b), Ph_2PCl (m).

Ph_2P–$P(SiMe_3)_2$ (0.32 mmol), $[(Et_2PhP)_2PtCl_2]$ (0.18 mmol): Et_2PhP (s), Ph_2P–PPh_2 (w), **B** (w), [{$(Et_2PhP)_2Pt$}$_2P_2$] (w), Polymer at +10 ppm (b), $Ph_2P(SiMe_3)$ (w), [(2,3-η-Ph_2PP=$PPPh_2$)$Pt(PPhEt_2)_2$] (m), Ph_2P–$P(SiMe_3)_2$ (s), Ph_2PCl (m).

Ph_2P–$P(SiMe_3)_2$(0.22 mmol), $[(EtPh_2P)_2PtCl_2]$ (0.21 mmol): $EtPh_2P$ (vs), [{$(EtPh_2P)_2Pt$}$_2P_2$] (m), polymer at +10 ppm (b).

Ph_2P–$P(SiMe_3)_2$ (0.31 mmol), $[(EtPh_2P)_2PtCl_2]$ (0.16 mmol): $EtPh_2P$ (vs), [{$(EtPh_2P)_2Pt$}$_2P_2$] (m), polymer at +10 ppm (b), Ph_2P–$P(SiMe_3)_2$ (s), $Ph_2P(SiMe_3)$ (m).

Ph_2P–$P(SiMe_3)_2$ (0.20 mmol), $[(p\text{-}Tol_3P)_2PtCl_2]$ (0.22 mmol): *p*-Tol_3P (vs), polymer at +20 ppm (b).

Ph_2P–$P(SiMe_3)_2$ (0.43 mmol), $[(p\text{-}Tol_3P)_2PtCl_2]$ (23 mmol): *p*-Tol_3P (vs), polymer at +20 ppm (b), Ph_2P–$P(SiMe_3)_2$ (s), $Ph_2P(SiMe_3)$ (m).

2.1.2. The ^{31}P NMR studies of the mixture obtained from the reaction of $(Et_2N)_2P$–$P(SiMe_3)_2$ with $[(R'_3P)_2PtCl_2]$

$(Et_2N)_2P$–$P(SiMe_3)_2$ reacts more slowly with $[(R'_3P)_2PtCl_2]$ than Ph_2P–$P(SiMe_3)_2$ (about 1 day). The ^{31}P NMR monitoring of the reaction mixtures is presented in Section 2.1.2. The main reaction path is **I**.

$(Et_2N)_2P$–$P(SiMe_3)_2$ (0.19 mmol), $[(Et_2PhP)_2PtCl_2]$ (0.20 mmol): Et_2PhP (s), $(Et_2N)_3P$ (s), [{$(Et_2PhP)_2Pt$}$_2P_2$] (s). We were not able to resolve many weak signals in the range from +37 to +22 ppm without Pt satellites.

$(Et_2N)_2P$–$P(SiMe_3)_2$ (0.35 mmol), $[(Et_2PhP)_2PtCl_2]$ (0.19 mmol): Et_2PhP (s), $(Et_2N)_2P$–$P(NEt_2)_2$ (m), [{$(Et_2PhP)_2Pt$}$_2P_2$] (s), $(Et_2N)_2P$–$P(SiMe_3)_2$ (m), $(Et_2N)_2P$–$P(SiMe_3)H$ (m), $(Et_2N)_3P$ (w). Many weak signals in the range from +37 to +24 ppm without Pt satellites we were not able to resolve.

$(Et_2N)_2P$–$P(SiMe_3)_2$ (0.19 mmol), $[(EtPh_2P)_2PtCl_2]$ (0.19 mmol): [{$(EtPh_2P)_2Pt$}$_2P_2$] (s), $P(NEt_2)_3$ (m), $PCl(NEt_2)_2$ (w), $EtPh_2P$ (w). Many weak signals in the range from +37 to +15 ppm without Pt satellites we were not able to resolve.

$(Et_2N)_2P$–$P(SiMe_3)_2$ (0.32 mmol), $[(EtPh_2P)_2PtCl_2]$ (0.16 mmol): [{$(EtPh_2P)_2Pt$}P_2] (s), $EtPh_2P$(w), $(Et_2N)_2P$–$P(SiMe_3)_2$ (s), $(Et_2N)_2P$–$P(SiMe_3)H$ (m), $(Et_2N)_2P$–$P(SiMe_3)$–$P(NEt_2)_2$ (w), $P(NEt_2)_3$ (w). Many weak signals in the range from +37 to +21 ppm without Pt satellites we were not able to resolve.

2.1.3. The ^{31}P NMR studies of the mixture obtained from the reaction of $(^iPr_2N)_2P$–$P(SiMe_3)_2$ with $[(R'_3P)_2PtCl_2]$

The reactions of $(^iPr_2N)_2P$–$P(SiMe_3)_2$ with $[(R'_3P)_2PtCl_2]$ were very slow. We did not observe any change in the mixture until the addition of the diphosphane was completed. Only after several hours at room temperature the mixture turned yellow and the suspension started to dissolve. After a few days the solution was clear and turned dark orange. The ^{31}P NMR monitoring of the reaction mixtures is presented in Section 2.1.3. The main reaction pathway is **I**, but products formed via the paths **II** and **III** are also visible. The resonances of $(^iPr_2N)_2PCl$ and $(^iPr_2N)_2P$–$P(N^iPr_2)_2$ are very strong. In case of a molar ratio $(^iPr_2N)_2P$–$P(SiMe_3)_2$:$[(R'_3P)_2PtCl_2]$ ($R'_3P = Et_2PhP$,*p*-Tol_3P) of 2:1 it is possible to isolate the related diphosphorus Pt complexes **1** and **2** as crystals in acceptable yield. With a molar ratio of 1:1 and $R'_3P = Et_3P$, the ionic complex [μ_2-(1,2:2-η-P_2){$Pt(PEt_3)_2$}$_2${$Pt(PEt_3)_2Cl$}]$^+Cl^-$ (**3**) could be isolated in a fairly good yield (Scheme 3). In the reaction solution we have not observed any ^{31}P NMR signals which can be attributed to **3**, presumably because this compound was formed in the final stages of reactions according to Scheme 3, or because of dynamic equilibria which can alter the ^{31}P NMR spectrum of this compound.

In the case of $R'_3P = Et_3P$ or Et_2PhP, ^{31}P NMR examinations of the reaction mixtures indicated two AA′XX′ spin systems (**C** and **E**). These reactions yield additionally some Pt complexes with five P atoms in the molecule (**D**, **F**, **G**, **H**, **I**, **K**) and a complex compound with four P atoms in the molecule (**L**).

$(^iPr_2N)_2P$–$P(SiMe_3)_2$ (0.28 mmol), $[(Et_3P)_2PtCl_2]$ (0.28 mmol): $(^iPr_2N)_2PCl$ (vs), $(^iPr_2N)_2P$–$P(N^iPr_2)_2$ (s), $(^iPr_2N)_2PH$ (m), [*trans*-$(Et_3P)_2PtCl_2$] (m), [*cis*-$(Et_3P)_2PtCl_2$] (m), Et_3P (m), **C** (m), **D** (m), $(^iPr_2N)_2P$–PH–$P(N^iPr_2)_2$ (m), [(2,3-η-{$(^iPr_2N)_2$)P–P=P–$P(N^iPr_2)_2$}$Pt(PEt_3)_2$] (w), [{$(Et_3P)_2Pt$}$_2P_2$] (w). The mixture appears to be very complex. We were not able to attribute many signals with Pt satellites especially in the range of 30–0 ppm (overlaps and higher order spectra).

$(^iPr_2N)_2P$–$P(SiMe_3)_2$ (0.34 mmol), $[(Et_3P)_2PtCl_2]$ (0.17 mmol): [{$(Et_3P)_2Pt$}$_2P_2$] (vs), $(^iPr_2N)_2P$–$P(N^iPr_2)_2$ (s), $(^iPr_2N)_2PCl$ (s), [(2,3-η-{$(^iPr_2N)_2$)P–P=P–$P(N^iPr_2)_2$}$Pt(PEt_3)_2$] (m), $(^iPr_2N)_2P$–$P(SiMe_3)H$ (w), $(^iPr_2N)_2P$–PH–$P(N^iPr_2)_2$ (w), **C** (w), **D** (w).

$(^iPr_2N)_2P$–$P(SiMe_3)_2$ (0.25 mmol), $[(Et_2PhP)_2PtCl_2]$ (0.25 mmol): $(^iPr_2N)_2PCl$ (vs), Et_2PhP (s), $(^iPr_2N)_2P$–$P(N^iPr_2)_2$ (s), [{$(Et_2PhP)_2Pt$}$_2P_2$] (s), $(^iPr_2N)_2PH$ (m), $(^iPr_2N)_2P$–PH–$P(N^iPr_2)_2$ (m), [(2,3-η-{$(^iPr_2N)_2$)P–P=P–$P(N^iPr_2)_2$}$Pt(PPhEt_2)_2$] (w), **E** (m), **F** (w), **G** (w). We have not resolved some signals with Pt satellites in the range of 18–2 ppm (overlaps and higher order spectra).

$(^iPr_2N)_2P$–$P(SiMe_3)_2$ (0.39 mmol), $[(Et_2PhP)_2PtCl_2]$ (0.18 mmol): $(^iPr_2N)_2P$–$P(N^iPr_2)_2$ (vs), [{$(Et_2PhP)_2Pt$}$_2P_2$] (m), $(^iPr_2N)_2PCl$ (m), $(^iPr_2N)_2PH$ (w), $(^iPr_2N)_2P$–PH–$P(N^iPr_2)_2$ (m), $(^iPr_2N)_2P$–$P(SiMe_3)_2$ (m), Et_2PhP(m), $(^iPr_2N)_2P$–$P(SiMe_3)H$ (w), $(^iPr_2N)_2P$–$P(SiMe_3)$–$P(N^iPr_2)_2$ (w).

$(^iPr_2N)_2P$–$P(SiMe_3)_2$ (0.25 mmol), $[(EtPh_2P)_2PtCl_2]$ (0.25 mmol): [{$(EtPh_2P)_2Pt$}$_2P_2$] (s), $(^iPr_2N)_2PCl$ (s), [*cis*-$(EtPh_2P)$){$(^iPr_2N)_2PH$}$PtCl_2$] (m), [*cis*-$(EtPh_2P)_2PtCl_2$] (m), $(^iPr_2N)_2P$–PH–$P(N^iPr_2)_2$ (m), $EtPh_2P$ (m), $(^iPr_2N)_2P$–$P(SiMe_3)H$ (w), **H** (w).

($^{i}Pr_2N)_2P–P(SiMe_3)_2$ (0.18 mmol), [$(EtPh_2P)_2PtCl_2$] (0.09 mmol): ($^{i}Pr_2N)_2P–P(N^{i}Pr_2)_2$ (s), ($^{i}Pr_2N)_2P–P(SiMe_3)H$ (s), ($^{i}Pr_2N)_2PCl$ (s), $EtPh_2P$ (s), ($^{i}Pr_2N)_2P–PH–P(N^{i}Pr_2)_2$ (m), ($^{i}Pr_2N)_2P–P(SiMe_3)_2$ (m), [{$(EtPh_2P)_2Pt$}$_2P_2$] (w).

($^{i}Pr_2N)_2P–P(SiMe_3)_2$ (0.25 mmol), [$(p\text{-}Tol_3P)_2PtCl_2$] (0.25 mmol): ($^{i}Pr_2N)_2P–P(N^{i}Pr_2)_2$ (vs), ($^{i}Pr_2N)_2PCl$ (s), ($^{i}Pr_2N)_2P–P(SiMe_3)H$ (s), ($^{i}Pr_2N)_2P–PH–P(N^{i}Pr_2)_2$ (s), *p*-Tol_3P (s), [{$(p\text{-}Tol_3P)_2Pt$}$_2P_2$] (m), [*cis*-$(p\text{-}Tol_3P)$\{($^{i}Pr_2N)_2PH$\}$PtCl_2$] (m), [$(p\text{-}Tol_3P)_2Pt\{\eta^2\text{-}(^{i}Pr_2N)_2P–P\}$] (w), **I** (w), polymer at +25 ppm (b,w).

($^{i}Pr_2N)_2P–P(SiMe_3)_2$ (0.50 mmol), [$(p\text{-}Tol_3P)_2PtCl_2$] (0.22 mmol): ($^{i}Pr_2N)_2P–P(N^{i}Pr_2)_2$ (s), ($^{i}Pr_2N)_2PCl$ (s), ($^{i}Pr_2N)_2P–P(SiMe_3)H$ (s), ($^{i}Pr_2N)_2P–PH–P(N^{i}Pr_2)_2$ (s), *p*-Tol_3P (s), [{$(p\text{-}Tol_3P)_2Pt$}$_2P_2$] (m), [*cis*-$(p\text{-}Tol_3P)$\{($^{i}Pr_2N)_2PH$\}$PtCl_2$] (m), [$(p\text{-}Tol_3P)_2Pt\{\eta^2\text{-}(^{i}Pr_2N)_2P–P\}$] (w), ($^{i}Pr_2N)_2P–P(SiMe_3)_2$ (m), **I** (w), **K** (w), **L** (w), polymer at +25 ppm (b,w).

2.1.4. The ^{31}P NMR studies of the mixture obtained from the reaction of $^{t}Bu_2P–P(SiMe_3)_2$ with [$(Et_2PhP)_2PtCl_2$]

The reaction between $^{t}Bu_2P–P(SiMe_3)_2$ and [$(Et_2PhP)_2PtCl_2$] was very slow. After several hours at room temperature the mixture turned yellow and the suspension started to dissolve. After a few days the mixture became transparent and turned dark orange. The ^{31}P NMR examinations of these reactions are listed in Section 2.1.4. These reactions yield products consistent with pathways **I** and **II** and additionally yield two complexes with four P atoms (**M** and **N**). The pathway **II** is visible only for $R_2P–P(SiMe_3)_2$ with sterically demanding R groups (R = ^{t}Bu or $^{i}Pr_2N$), but pathway **I** clearly predominates. It is probably a substitution of Cl in [$(R'_3P)_2PtCl_2$] by means of $R_2P–P(SiMe_3)_2$ with two eliminations of Me_3SiCl molecules (Scheme 2).

$^{31}P\{^{1}H\}$ NMR of **M** is in accord with the proposed formula for the intermediate complex (*). In the case of R = $^{i}Pr_2N$ and R'_3P = *p*-Tol_3P there is such a conformity for compound **L** (see supplementary material).

$^{t}Bu_2P–P(SiMe_3)_2$ (0.22 mmol), [$(Et_2PhP)_2PtCl_2$] (0.21 mmol): [{$(Et_2PhP)_2Pt$}$_2P_2$] (s), $^{t}Bu_2PH$ (s), Et_2PhP (s), $^{t}Bu_2PCl$ (w), [$(Et_2PhP)_2Pt(\eta^2\text{-}^{t}Bu_2P–P)$] (m), $^{t}Bu_2P–P^{t}Bu_2$ (w), **M** (w), **N** (w), $P(P^{t}Bu_2)_3$ (w).

$^{t}Bu_2P–P(SiMe_3)_2$ (0.47 mmol), [$(Et_2PhP)_2PtCl_2$] (0.23 mmol): [{$(Et_2PhP)_2Pt$}$_2P_2$] (s), $^{t}Bu_2PH$ (s), Et_2PhP (s), $^{t}Bu_2PCl$ (w), [$(Et_2PhP)_2Pt(\eta^2\text{-}^{t}Bu_2P–P)$] (m), $^{t}Bu_2P–P^{t}Bu_2$ (w), **M** (w), **N** (w), $^{t}Bu_2P–P(SiMe_3)_2$ (vs), $^{t}Bu_2P–P(SiMe_3)H$ (m), $P(P^{t}Bu_2)_3$ (w).

2.2. ^{31}P NMR studies of reaction products

The ^{31}P NMR data of the known compounds are given in the supplementary material. The $^{31}P\{^{1}H\}$ NMR data for the diphosphorus complexes [{$(R'_3P)_2Pt$}$_2P_2$] are summarized in Table 1, for the tetraphosphene complexes [$(R'_3P)_2Pt(2,3\text{-}\eta\text{-}R_2P{=}P{=}PR_2)$] in Table 2. Table 3 showing the data for Pt complexes with five P atoms (not completely) and Table 4 showing the data for Pt complexes with four P atoms are in the supplementary material. The $^{31}P\{^{1}H\}$ NMR data for the unknown compounds **A**–**E** are in the supplementary material.

2.3. X-ray crystallographic studies

Complex **1** crystallized in the orthorhombic system, space group *Pbca*. The molecular structure of [{$(Et_2PhP)_2Pt$}$_2P_2$] (**1**) is shown in Fig. 1. Complex **2** crystallized in the monoclinic system, space group *C*2/*c*. The molecular structure of [{$(p\text{-}Tol_3P)_2Pt$}$_2P_2$]·$2Et_2O$ (**2**) is shown in Fig. 2. The structures of **1** and **2** are similar to that of [{(depe)Ni}$_2P_2$] [2]. The molecule of **1** consists of two distorted square-planar arrangements P1–P2–P5–P6–Pt1 and P3–P4–P5–P6–Pt2 respectively, almost perpendicular to each other, which form a "roof" framework. The geometry of such a $PtP_2(ML_n)_2$ system (ML_n 14 VE) can be viewed as a result of a π donor interaction of four electrons of a P_2 molecule to two $d^{10}ML_2$ metal centers. The dihedral angle between these planes (99.75°) illustrates the approximate orthogonality of the two π bonds in the triple bond of the P_2 unit. The P5–P6 distance in the P_2 group (214.1 pm) lies between the values for a P=P bond in sterically protected diphosphenes (≈203 pm) [11] and the typical values for a single P–P bond (≈ 220 pm). The PtP_4 systems (P1–P2–Pt1–P5–P6) and (P3–P4–Pt2–P5–P6) are almost planar, with a root mean square deviation of fitted atoms from planarity of 5.79 pm and 7.55 pm, respectively.

The asymmetric unit of **2** contains half of the complex molecule and two halves of diethyl ether molecules. The centre of the diphosphorus ligand sits on a twofold rotation axis (Wyckoff position ***e***) [12]. The dihedral angle between the planes (Pt1–P3–P3#1) and (Pt1#1–P3–P3#1) is a bit larger than in the case of **1** and equals to 104.37(7)°, probably due to packing effects. The platinum atom Pt1 adopts a distorted square-planar coordination with a root mean square deviation of fitted atoms of 6.60 pm from the mean plane (P1–P2–Pt1–P3–P3#1). The other plane has the same geometry as both are symmetry equivalent. The bond

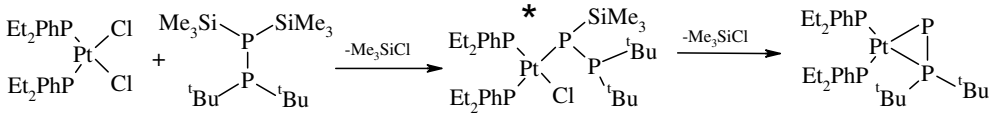

Scheme 2. Proposed reaction sequence on pathway **II**.

Table 1
$^{31}P\{^{1}H\}$ NMR data of $[\{(R'_3P)_2Pt\}_2P_2]$: P1,2,3,4 = R′$_3$P, P1,2 = P_2

	δP1,2,3,4 ($^1J_{Pt-P}$)	δP5,6 ($^1J_{Pt-P}$)	Peak distance
$[\{(Et_3P)_2Pt\}_2P_2]$ [1]	pst 10.7 (3487)	psq 47.2 (0–5)	22.9
$[\{(Et_2PhP)_2Pt\}_2P_2]$ (**1**)	pst 11.1 (3506)	psq 48.7 (0–5)	22.8
$[\{(EtPh_2P)_2Pt\}_2P_2]$	pst 16.5 (3588)	psq 55.7 (0–5)	22.9
$[\{(p\text{-}Tol_3P)_2Pt\}_2P_2]$ (**2**)	pst 21.6 (3602)	psq 99.0 (27)	25.2

AA′XX′A″A‴ – pattern, pst – pseudotriplet; psq – pseudoquintet, peak distance – the apparent coupling constants in the pseudo multiplets (see Section 2.4).

Table 2
$^{31}P\{^{1}H\}$ NMR data of $[(R'_3P5,6)_2Pt(2,3\text{-}\eta\text{-}R_2P1\text{–}P2{=}P3\text{–}P4R_2)]$

	δP1,4 ($^1J_{Pt-P}$)	δP2,3($^1J_{Pt-P}$)	δP5,6 ($^1J_{Pt-P}$)
$[(Et_3P)_2Pt(2,3\text{-}\eta\text{-}Ph_2PP{=}PPPh_2)]$	−12.3 (46)	−36.4 (284.6)	18.8 (3262)
$[(Et_2PhP)_2Pt(2,3\text{-}\eta\text{-}Ph_2PP{=}PPPh_2)]$	−12.1 (38)	−31.5 (289,0)	16.0 (3267)
$[(Et_3P)_2Pt(2,3\text{-}\eta\text{-}(^iPr_2N)_2PP{=}PP(N^iPr_2)_2\}]$	87. 0 (55)	−4.4 (229.5)	16.5 (3254)
$[(Et_2PhP)_2Pt\{2,3\text{-}\eta\text{-}(^iPr_2N)_2PP{=}PP(N^iPr_2)_2\}]$	85.9 (62)	−4.4 (242)	16.8 (3265)

AA′MM′XX′ – pattern, for $[(R_3P)_2Pt[(2,3\text{-}\eta\text{-}^tBu_2PP){=}PP^tBu_2]]$ (R_3P = Ph_3P, $EtPh_2P$) see [10].

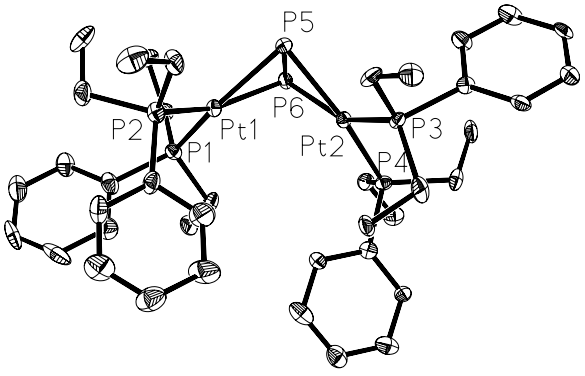

Fig. 1. The molecular structure of $[\{(Et_2PhP)_2Pt\}_2P_2]$ (**1**). Displacement ellipsoids 50%, hydrogen atoms not shown.

length between the phosphorus atoms in the bridging P_2 unit is short (211.0(6) pm), similar as in **1**.

Compound **3** crystallized in the monoclinic system (space group $P2_1/c$). The molecular structure of $[\mu_2\text{-}(1,2{:}2\text{-}\eta\text{-}P_2)\{Pt(PEt_3)_2\}_2\{Pt(PEt_3)_2Cl\}]^+Cl^-$ (**3**) is shown in Fig. 3.

$[\{(Et_3P)_2Pt\}_2P_2]$ is coordinated terminally to the $(Et_3P)_2PtCl^+$ moiety via a lone pair of the P_2 group. This additional terminal coordination exerts only minor influence on the geometry of the "roof" skeleton P7–P8–Pt3–P2–P1–Pt1–P3–P4. The distance P1–Pt2 of 234.3(4) pm is relatively long. It is in the range typical for $[trans\text{-}(PR_3)_2PtCl_2]$. For terminally bonded phosphaalkene $[cis\text{-}PtCl_2(PEt_3)(\eta^1\text{-}MesP\text{-}CPh_2)]\cdot CHCl_3$ [13] the related Pt–P distance is much shorter (219.9 pm). The P1–P2 distance of 212.9(5) pm is similar as in **1** or in **2**. The coordination P1–Pt2 causes a widening of the torsion angle

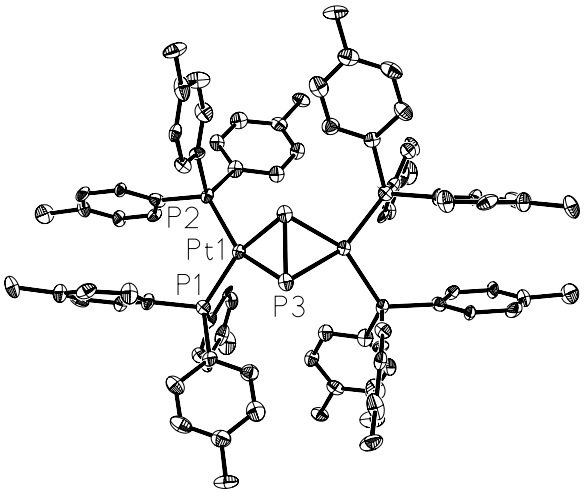

Fig. 2. The molecular structure of $[\{(p\text{-}Tol_3P)_2Pt\}_2P_2]\cdot 2Et_2O$ (**2**). Displacement ellipsoids 50%, two solvent Et_2O molecules and hydrogen atoms not shown.

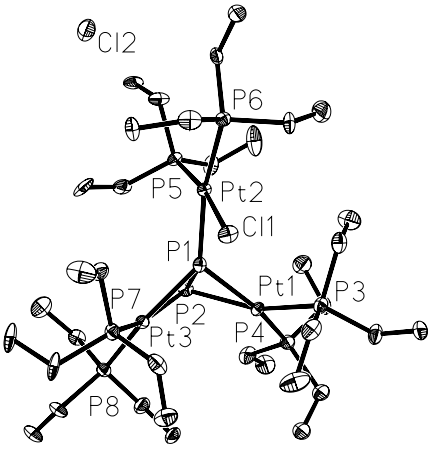

Fig. 3. Molecular structure of $[\mu_2\text{-}(1,2{:}2\text{-}\eta\text{-}P_2)\{Pt(PEt_3)_2\}_2\{Pt(PEt_3)_2\text{-}Cl\}]^+Cl^-$ (**3**), showing non-carbon atoms labeling. Displacement ellipsoids 50%, hydrogen atoms not shown.

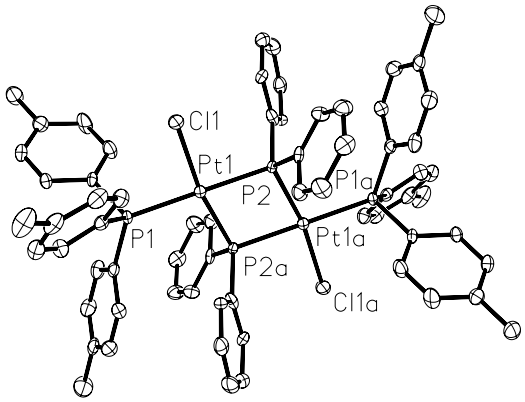

Fig. 4. Molecular structure of [(*p*-Tol$_3$P)ClPt(μ-PPh$_2$)$_2$Pt(*p*-Tol $_3$P)Cl] (**4**). Displacement ellipsoids 50%, hydrogen atoms not shown, symmetry code *a*: 2 − x, 1 − y, −z.

Pt1–P1–P2–Pt3 (110.41°) as compared to 99.13° in **1**. The Pt2–P6 distance of 236.5(4) pm is distinctly longer than Pt2–P5 (224.2(4) pm) due to a *trans* effect of the P1–Pt2 bond. The distance Pt1–Pt3 (347.2 pm) clearly indicates no Pt–Pt bonding. For Pt(I) dimers with bridging phosphido ligands Pt–Pt distances of about 260 pm were reported [14].

[(*p*-Tol$_3$P)ClPt(μ-PPh$_2$)$_2$Pt(*p*-Tol$_3$P)Cl] (**4**) crystallized in the triclinic system, space group $P\bar{1}$ (Fig. 4). It is the second reported phosphido-bridged complex of Pt(II), similar to [(^{t}Bu$_2$PH)ClPt(μ- PPh$_2$)$_2$Pt(^{t}Bu$_2$PH)Cl] [15].

The molecule is centrosymmetric with a centre of symmetry placed inside the Pt$_2$P$_2$ ring. The Pt1–P2–Pt1a–P2a ring is planar with a Pt1–Pt1a distance of 351.8 pm which indicates no Pt–Pt bonding. Cl*1* and Cl*1a* are in *trans* position imposed by the symmetry center. The coordination environment of Pt is planar, the sum of valence angles around Pt1 is 359.9°. The Pt1–P2 bond of 233.2(2) pm is remarkably longer than Pt1–P2a (227.0(2) pm), which illustrates the significant *trans* effect of (*p*-Tol)$_3$P compared to the Cl$^-$ ligand.

2.4. The ^{31}P NMR spectra of *1–3*

Compounds **1** and **2** are AA′XX′A″A‴ systems (Table 1), and their ^{31}P{^{1}H} NMR spectra are very similar to [{(Et$_3$P)$_2$Pt}$_2$P$_2$] [1]. Both the pseudo quintet and the pseudo triplet have small and partly hidden lines of satellite spectra in the signal basis, but only the pseudo triplet shows satellite peaks with $^1J_{Pt-P}$ of the usual size. The peak distances in the pseudo multiplets give the mean value $(^2J_{AX} + {}^2J_{A'X})/2$ and are not coupling constants. These are strongly correlated and therefore cannot be directly evaluated. The line width of the peaks in the main multiplets are about 4–5 Hz which is just the same order of

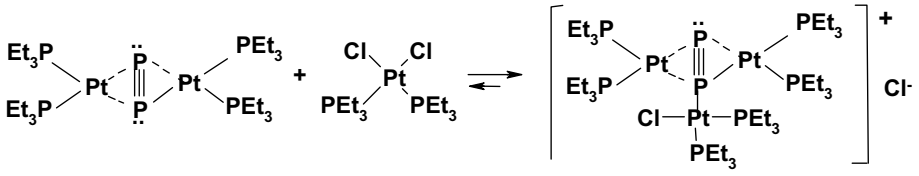

Scheme 3. The formation of complex **3**.

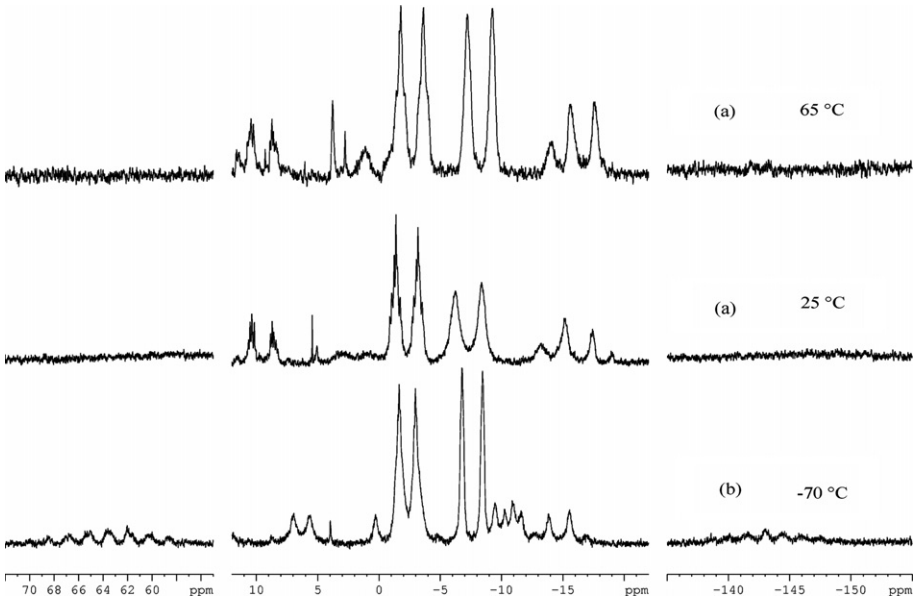

Fig. 5. Temperature dependant ^{31}P{^{1}H} NMR spectra of **3** in THF–C$_6$D$_6$ solution; recorded (a) on Bruker AMX300 and (b) on Bruker Av400.

magnitude as in peaks of some phosphanes also present in the samples.

The formation of **3** can be seen as a coordination of $[\{(Et_3P)_2Pt\}_2P_2]$ via the lone electron pair of the P_2 ligand to [*cis*-$(Et_3P)_2PtCl_2$] according to Scheme 3.

The $^{31}P\{^1H\}$ NMR spectrum of a solution of crystals of **3** in THF and C_6D_6 contained very small amounts of unknown Pt–P compounds, however no signals of [*cis*-$(Et_3P)_2PtCl_2$] nor of $[\{(Et_3P)_2Pt\}_2P_2]$ could be identified. Quite contrary to them and to **1** and **2**, the main signals in this spectrum have line widths of about 60–90 Hz at ambient temperature. No fine structure is resolved, just two "doublets" accompanied by ^{195}Pt satellites and two additional very broad signals without ^{195}Pt satellites can be recognized. These "doublets" must be assigned to P3 and P7 as well as to P4 and P8 of **3**, and the broad signals to P1 and P2. The peaks for P5 and P6 must be hidden by the large "doublets". Anyway, it is not possible to assign the spectrum unequivocally to the structure of **3**.

In order to identify the multiplets and to test for dynamic processes involving **3**, spectra on two spectrometers with different basis frequencies and at various temperatures were recorded (Fig. 5). At −70 °C and −30 °C the resonances of P1 (≈−143 ppm) and P2(≈+65 ppm) slightly resolve to multiplet patterns, however the line widths in the other parts of the spectra do not really narrow. At +50 °C the multiplet at about −2.5 ppm gets somewhat better resolved, but already at +65 °C this is lost again, probably due to a considerable amount of decomposition of **3**. There is also some minor temperature shift over the observed range. It was not possible to freeze any isomers of **3** nor to reach a sufficiently fast process to get narrow line spectra. It can be assumed, but so far not verified, that the $Pt3(PEt_3)_2Cl$ unit migration between P1 and P2 of **3** is at least part of the dynamic process.

3. Conclusions

The silylated diphosphanes $R_2P–P(SiMe_3)_2$ react with complexes of platinum $[(R'_3P)_2PtCl_2]$ in a complex way. The main path is connected with a splitting of the P–P bond of the $R_2P–P(SiMe_3)$ moiety leading in a sequence of reactions (including recombination steps of building blocks) to diphosphorus complexes of platinum(0) of the type $[(L_2Pt)_2P_2]$. ^{31}P NMR examinations of the reaction solutions indicate a formation of many other compounds resulting from the reactions of the released R_2P fragment (probably radical), i.e. $R_2P–PR_2$, R_2PCl, R_2PH, R_2PSiMe_3, $[(R'_3P)ClPt(\mu\text{-}PPh_2)_2Pt(PR'_3)Cl]$, $R_2P–P(SiMe_3)–PR_2$, and $R_2P–PH–PR_2$, $(Et_2N)_3P$ and $P(P^tBu_2)_3$.

In those reactions of diphosphanes $R_2P–P(SiMe_3)_2$, where R are sterically demanding groups like ^{t}Bu or $^i Pr_2N$, with $[(R'_3P)_2PtCl_2]$, we establish a formation of phosphino-phosphinidene complexes $[(R'_3P)_2Pt(\eta^2\text{-}R_2P–P)]$ [16] in poor yield together with complex mixtures of other compounds. This is a striking difference as compared to the reactions of $R_2P–P(SiMe_3)Li$ with $[(R'_3P)_2PtCl_2]$ which proceed under formation of these complexes in a fairly good yield [17].

4. Experimental

4.1. General comments

All reactions and manipulations were carried out under an atmosphere of ultra-high purified argon employing standard Schlenk techniques. Solvents were purified, dried and distilled prior to use from dark blue potassium or sodium diphenyl ketyl solution [18]. The known diphosphanes $R_2P–P(SiMe_3)_2$ (R = Ph, ^{t}Bu, Et_2N) were prepared according to published methods [19–21], $(^iPr_2N)_2P–P(SiMe_3)_2$ was prepared according to the published method for $(Et_2N)_2P–P(SiMe_3)_2$ [21]. $[(R'_3P)_2PtCl_2]$ ($R'_3P = Me_3P$, Et_3P, Et_2PhP, $EtPh_2P$ and p-Tol_3P) were prepared according to procedures described in [22].

^{31}P NMR spectra were recorded on Bruker AC250, Bruker Av400, Bruker AMX300 and Varian Unity+ 500 spectrometers (external standard 85% H_3PO_4) mainly at ambient temperature. For compound **3** variable temperature NMR studies were performed.

All reactions of $R_2P–P(SiMe_3)_2$ with $[(R'_3P)_2PtCl_2]$ were carried out in the same way. Therefore, only those runs which resulted in well defined crystalline products are described more detailed.

4.2. Synthesis of $[\{(Et_2PhP)_2Pt\}_2P_2]$ (1)

Compound **1** was obtained in a reaction between $(^iPr_2N)_2P–P(SiMe_3)_2$ and $[(Et_2PhP)_2PtCl_2]$ in the molar ratio of 2:1. To a stirred slurry of $[(Et_2PPh)_2PtCl_2]$ (107 mg, 0.18 mmol) in THF (2 ml) at −40 °C was slowly dropped $(^iPr_2N)_2P–P(SiMe_3)_2$ (159 mg, 0.39 mmol) dissolved in THF (2 ml). The mixture was allowed to warm to room temperature and was stirred for 4 days. The suspension dissolved and the solution turned orange. The solution was examined with ^{31}P NMR, then evaporated under vacuum (1 mTorr, 3 h). The residue was dissolved in pentane (3 ml) and filtered. After one month at +4 °C small pale-yellow crystals of **1** deposited (33 mg, 0.030 mmol). **1** is for short time stable in air. ^{31}P NMR (see Table 1). Anal. Calc. for $C_{40}H_{60}P_6Pt_2$: C, 43.02; H, 5.42. Found: C, 43.31; H, 5.57%.

4.3. Synthesis of $[\{(p\text{-}Tol_3P)_2Pt\}_2P_2] \cdot 2Et_2O$ (2)

Compound **2** is a product of the reaction of $(^iPr_2N)_2P–P(SiMe_3)_2$ with $[(p\text{-}Tol_3P)_2PtCl_2]$ in a molar ratio of 2:1. To a stirred slurry of $[(p\text{-}Tol_3P)_2PtCl_2]$ (150 mg, 0.22 mmol) in THF (1.5 ml) at −40 °C was slowly dropped $(^iPr_2N)_2P–P(SiMe_3)_2$ (204 mg, 0.50 mmol) dissolved in THF (1.5 ml). The mixture was allowed to warm to room temperature and stirred for 3 days. The suspension dissolved and the solution turned dark brown. The solution was examined with ^{31}P NMR, then evaporated under vacuum

(1 mTorr, 5 h). The residue was dissolved in diethyl ether (5 ml), filtered and evaporated to 1 ml. After one month at +4 °C a small amount of thin pale-yellow needles of **2** deposited. Compound **2** is for short time stable in air. ^{31}P NMR see Table 1.

4.4. Synthesis of $[\mu_2$-(1,2:2-η-$P_2)\{Pt(PEt_3)_2\}_2\{Pt(PEt_3)_2Cl\}]^+Cl^-$ (3)

Compound **3** is a product of the reaction of $(^iPr_2N)_2P$–$P(SiMe_3)_2$ with $[(Et_3P)_2PtCl_2]$ in a molar ratio of 1:1. To a stirred slurry of $[(Et_3P)_2PtCl_2]$ (144 mg, 0.28 mmol) in THF (2 ml) at −40 °C was slowly dropped $(^iPr_2N)_2P$–$P(SiMe_3)_2$ (114 mg, 0.28 mmol) dissolved in THF (2 ml). The mixture was allowed to warm to room temperature and stirred for 4 days. The suspension dissolved and the solution turned orange. The solution was examined by ^{31}P NMR (very complex mixture), then evaporated under vacuum (1 mTorr, 1 h). The residue was dissolved in pentane (5 ml), filtered and concentrated to ≈ 1 ml. After 2 months at ambient temperature big, almost colorless crystals of **3** were obtained (≈50 mg, 0.035 mmol). Compound **3** is moderately stable in air.

^1H NMR (THF–C_6D_6, 295 K): 1.99–1.86 m, overlapped PCH_2CH_3; 1.02–0.92 m, overlapped PCH_2CH_3. ^{31}P NMR (THF–C_6D_6, 203 K): 63.4, m, P1, $^1J_{Pt-P} \approx 0$; −2.3, m, P3, P7, $^1J_{Pt1-P3} \approx 2780$; −2.3, m, P5, $^1J_{Pt3-P5} \approx 2700$; −7.8, m, P4, P8, $^1J_{Pt1-P4} \approx 2300$; −10.2, m, P5, $^1J_{Pt3-P5} \approx 2700$; −142.9, m, P2, $^1J_{Pt1-P2} \approx 0$; small signals at 23.11 ppm (s, no $^1J_{P-H}$, $^1J_{Pt-P} = 2710$ Hz) not detected in the reaction mixture and at 20.22 ppm (d, 22.8 Hz, no $^1J_{P-H}$, $^1J_{Pt-P} = 2605$ Hz) detected in the reaction mixture. Anal. Calc. for $C_{36}H_{90}P_8Pt_3Cl_2$: C, 30.30; H, 6.36. Found: C, 30.62; H, 6.12%.

4.5. Synthesis of $[(p\text{-}Tol_3P)ClPt(\mu\text{-}PPh_2)_2Pt(p\text{-}Tol_3P)Cl]$ (4)

Compound **4** is a product of the reaction Ph_2P–$P(SiMe_3)_2$ with $[(p\text{-}Tol_3P)_2PtCl_2]$ in molar ratio 1:1. To a stirred slurry of $[(p\text{-}Tol_3P)_2PtCl_2]$ (150 mg, 0.22 mmol) in THF (1.5 ml) at −40 °C was slowly dropped Ph_2P–$P(SiMe_3)_2$ (74 mg, 0.204 mmol) dissolved in THF (1.5 ml). After warming up the mixture to room temperature it turned immediately orange and the suspension dissolved. After 2 days the solution was examined with ^{31}P NMR, then evaporated under vacuum (1 mTorr, 5 h). The residue was dissolved in toluene (5 ml), filtered and evaporated to 0.5 ml. After one week at ambient temperature 3 ml pentane was added to the toluene solution. After 4 months a small amount of very thin colorless crystals of **4** was obtained.

4.6. Crystal structure determinations

Diffraction data were collected at 100 K (**1**) and 120 K (**2**–**4**) on a KUMA KM4CCD diffractometer, Oxford Diffraction Ltd. Numerical absorption correction based on the multi-faceted crystal shape with empirical scaling was applied (CrysAlis RED, Oxford Diffraction [23,24]). Details of crystal data, data collection and refinement are summarized in Table 6 (supplementary material). The structures were solved by direct methods using the SHELX-97 program package [25,26] and refined with full-matrix least-squares on F^2. All atoms, excluding hydrogen, were refined with anisotropic displacement ellipsoids. Carbon atom C33 from the ethyl group in compound **1**, due to its tendency to become non-positively defined, had to be refined isotropically. In the case of **2**, solvating diethyl ether molecules were refined using an isotropic model with constrained bond lengths. Hydrogen atoms were positioned geometrically and refined as riding on their heavy atoms.

Acknowledgements

W.D.-B. and J.P. thank the Polish State Committee of Scientific Research (project No. 1 T09A 148 30) for financial support.

Appendix A. Supplementary material

CCDC 609987, 609988, 616584 and 616585 contain the supplementary crystallographic data for compounds **1**–**4**. These data can be obtained free of charge via http://www.ccdc.cam.ac.uk/conts/retrieving.html, or from the Cambridge Crystallographic Data Centre, 12 Union Road, Cambridge CB2 1EZ, UK; fax: (+44) 1223-336-033; or e-mail: deposit@ccdc.cam.ac.uk.

The ^{31}P NMR data of the discussed compounds and details of the crystal structure determinations of **1**–**4** are available from the authors on request. Supplementary data associated with this article can be found, in the online version, at doi:10.1016/j.jorganchem.2007.04.045.

References

[1] H. Schäfer, D. Binder, Z. Anorg. Allg. Chem. 560 (1988) 65.
[2] H. Schäfer, D. Binder, D. Fenske, Angew. Chem. 97 (1985) 523; H. Schäfer, D. Binder, D. Fenske, Angew. Chem. Int. Ed. Eng. 24 (1985) 522.
[3] H. Schäfer, D. Binder, B. Deppisch, G. Mattern, Z. Anorg. Allg. Chem. 546 (1987) 79.
[4] H. Krautscheid, E. Matern, I. Kovacs, G. Fritz, J. Pikies, Z. Anorg. Allg. Chem. 623 (1997) 1917.
[5] J. Olkowska-Oetzel, J. Pikies, Appl. Organometal. Chem. 17 (2003) 28.
[6] J. Pikies, E. Baum, E. Matern, J. Chojnacki, R. Grubba, A. Robaszkiewicz, J. Chem. Soc. Chem. Commun. (2004) 2478.
[7] E. Baum, E. Matern, A. Robaszkiewicz, J. Pikies, Z. Anorg. Allg. Chem. 632 (2006) 1073.
[8] J-P. Bezombes, K.B. Borisenko, P.B. Hitchcock, M.F. Lappert, J.E. Nycz, D.W.H. Rankin, H.E. Robertson, J. Chem. Soc. Dalton. Trans. (2004) 1980.
[9] C. Eaborn, K.J. Odell, A. Pidcock, J. Organomet. Chem. 170 (1979) 105.
[10] H. Krautscheid, E. Matern, G. Fritz, J. Pikies, Z. Anorg. Allg. Chem. 626 (2000) 253.

[11] A.H. Cowley, Polyhedron 3 (1984) 389.
[12] T. Hahn (Ed.), International Tables for Crystallography, vol. C, Kluwer Academic Publishers, Dordrecht, The Netherlands, 2002.
[13] H.W. Kroto, J.F. Nixon, M.T. Taylor, A.F. Frew, K.W. Muir, Polyhedron 1 (1982) 89.
[14] C. Mealli, A. Ienco, A. Galandino, E.P. Carreňo, Inorg. Chem. 38 (1999) 4620.
[15] A.J. Carty, F. Hartstock, V.J. Taylor, Inorg. Chem. 21 (1982) 1349.
[16] E. Matern, J. Pikies, G. Fritz, Z. Anorg. Allg. Chem. 626 (2000) 2136.
[17] W. Domańska, J. Pikies, VIIth Polish Symposium of Heteroorganic Chemistry PTChem, Łódź 25.11.2004.
[18] W.L.F. Armarego, D.D. Perrin, Purification of Laboratory Chemicals, Butterworth-Heinemann, Oxford, 1997.
[19] G. Fritz, T. Vaahs, J. Härer, Z. Anorg. Allg. Chem. 552 (1987) 11.
[20] G. Fritz, W. Hölderich, Z. Anorg. Allg. Chem. 431 (1977) 76.
[21] I. Kovacs, E. Matern, G. Fritz, Z. Anorg. Allg. Chem. 622 (1996) 935.
[22] F.R. Hartley, Organometal. Chem. Rev. A 6 (1970) 119.
[23] Oxford Diffraction, 2005. CrysAlis CCD and CrysAlis RED. Version 1.171. Oxford Diffraction Ltd., Abingdon, Oxfordshire, England.
[24] R.C. Clark, J.S. Reid, Comput. Phys. Commun. 111 (1998) 243.
[25] G.M. Sheldrick, SHELXS97. Program for Crystal Structure Solution, University of Göttingen, Germany, 1997.
[26] G.M. Sheldrick, SHELXL97. Program for Crystal Structure Refinement, University of Göttingen, Germany, 1997.